Transition states for hydride–water (H−)(H2O)n clusters, n=2–6, 20

ARTICLE *in* JOURNAL OF MOLECULAR STRUCTURE THEOCHEM · DECEMBER 2008

Impact Factor: 1.37 · DOI: 10.1016/j.theochem.2009.09.012

2 AUTHORS, INCLUDING:

David Anick
Tufts University, Medford, MA, United States
78 PUBLICATIONS **2,049** CITATIONS

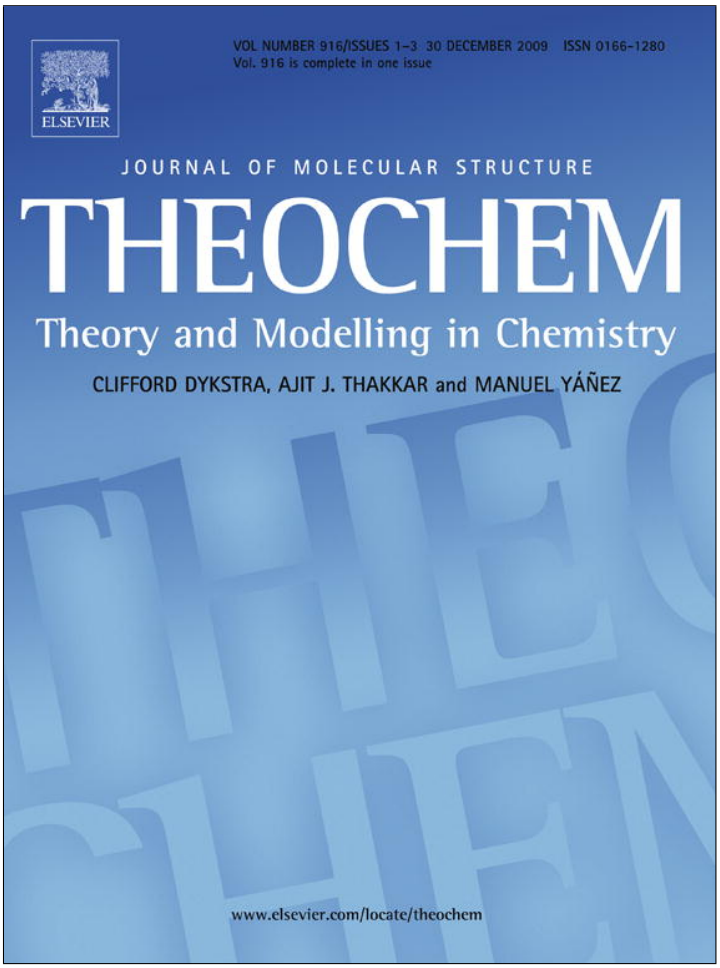

Journal of Molecular Structure: THEOCHEM 916 (2009) 61–71

Contents lists available at ScienceDirect

Journal of Molecular Structure: THEOCHEM

journal homepage: www.elsevier.com/locate/theochem

Transition states for hydride-water $(H^-)(H_2O)_n$ clusters, $n = 2–6, 20$

David J. Anick [a,*], Kevin Leung [b]

[a] Harvard Medical School, 115 Mill St., Belmont, MA 02478, USA
[b] Sandia Laboratories, MS 1415, Albuquerque, NM 87185, USA

ARTICLE INFO

Article history:
Received 27 July 2009
Received in revised form 3 September 2009
Accepted 4 September 2009
Available online 11 September 2009

Keywords:
Hydride
Water cluster
Dodecahedral cage
AIMD
Laage–Hynes move

ABSTRACT

Hydride anion (H^-) reacts quickly in aqueous solution to form molecular hydrogen (H_2) and hydroxide ion (OH^-), but $(H^-)(H_2O)_n$ clusters have many PES local minima in which the hydride is solvated by two or more water molecules making dihydrogen bonds. Using *ab initio* methods applied to $(H^-)(H_2O)_n$ clusters for $n \leqslant 6$ and for $n = 20$, we explored these clusters' reaction pathways and transition states. At the B3LYP/6−311++G** level of theory, all of the small ($2 \leqslant n \leqslant 6$) clusters are unstable or barely stable at 0 K: all activation barriers for reaction to form H_2 are under 0.5 kcal/mol, all but one are under 0.2 kcal/mol, and most are negative. In some instances the lowest-barrier reaction pathway is multi-step, requiring H-bond rearrangements first, and those rearrangements are consistent with improving the "presolvation" of the emerging (OH^-) in accordance with a "solvation hierarchy." The arrangements explored for $n = 20$ consist of (H^-) encapsulated by a dodecahedral cage with coordination of 3, 4, 5, or 6 at the hydride anion. The lowest-energy $(H^-)(H_2O)_{20}$ cluster found has 4 H-bonds to the anion. Of several reaction pathways explored, the lowest barrier height is 3.68 kcal/mol at 0 K, suggesting that a low-temperature stable solvated hydride can exist. For the $(H^-)(H_2O)_{20}$ clusters at their transition states to H_2 formation, the H^-–H distances are at or below the van der Waals cutoff for covalent H—H bonding (92 pm). In all, 21 transition states to $(H_2)(OH^-)(H_2O)_{n-1}$ and eight H-bond rearranging transition states are presented. During a 25 ps AIMD simulation of H^- in a box of 32 H_2O's at 300 K, reaction to form H_2 did not occur, the hydride ion spent 95% of the time being 4-coordinated, and two first-shell exchanges were observed. This and other calculations suggest the mean survival time of (H^-) in bulk water at 300 K is likely between 20 and 100 ps.

1. Introduction

Understanding of hydride-water interactions is important for biological energy metabolism, fuel cell studies and nuclear materials research. In aqueous context, hydride transfer occurs during the formation of NADH from NAD^+ in the Krebs cycle [1], and Makoto [2] noted that solvation by a water cluster can lower the activation energy for H^- transfer in acycloin anions by 10 kcal/mol. Stable aqueous hydride anion has not been directly observed but there may be a steady-state population of short-lived solvated hydrides in some electrolysis systems [3,4]. Metal hydrides react quickly and irreversibly with water to produce dihydrogen gas and metal hydroxide. The interaction of solid LiH with bulk water to produce LiOH and H_2 has been extensively modeled as a two-step process [5–7]. The actual chemical reaction

$$(H^-)_{aq} + H_2O \rightarrow (H_2)_g + (OH^-)aq \quad (1)$$

is rapid, but it soon creates a surface-adjacent layer of dissolved LiOH that acts as a barrier, and then diffusion of water toward the surface and LiOH away from it become the rate-limiting first step.

The project described here used *ab initio* methods to study the reaction (1) in small and medium size water clusters. Lee et al. [8] demonstrated that $(H^-)(H_2O)_n$ clusters can have multiple PES local minima for $n \leqslant 6$, but for $n > 1$ they did not look at transition states. We were particularly interested in assessing the transition energy barriers for (1) in clusters and exploring whether any structural attributes of $(H^-)(H_2O)_n$ clusters might render them longer-lived. Interestingly, for $n = 1$, i.e. reaction (1) in gas phase, the reaction is endothermic [9]. The global minimum geometry for $(H_3O)^-$ has H^- solvated by one H_2O, but for $n \geqslant 2$, where the hydroxide ion can be solvated by one or more H_2O's, (1) becomes exothermic and the global minimum has the form $(H_2)(OH^-)(H_2O)_{n-1}$. At PES local minima for $n \geqslant 2$, $(H^-)(H_2O)_n$ clusters have the anion solvated by two or more H_2O units forming dihydrogen bonds [10]. Characteristics of the H–H interaction in dihydrogen bonds, including its length range and correlation of length with O–H stretch frequency, are similar to those of other O–H - - X hydrogen bonds [11–13].

* Corresponding author. Tel.: +1 6178552131; fax: +1 6174922002.
E-mail address: david.anick@rcn.com (D.J. Anick).

0166-1280/$ - see front matter © 2009 Elsevier B.V. All rights reserved.
doi:10.1016/j.theochem.2009.09.012

Kelly and Rosseinsky [4] used a variety of methods to predict properties of the short-lived solvated H^- species. They particularly noted the similarity of solvated H^- to solvated F^-. Bringing several experimental methods to bear on the question, their estimates for the ratio of H^- radius to F^- radius, $\rho(H^-/F^-)$, ranged from 1.03 to 1.09. The pKa of H_2 in H_2O was estimated to be 22 ± 2 at 25 °C. Gibbs free energy of formation of H^- in aqueous solution $\Delta_f G^0$ was found to be 141 ± 4 kJ/mol at 25 °C, while free energy of solvation (from gas phase at STP into H_2O) was found to be −421 ± 4 kJ/mol at 25 °C.

The similarity of H^- to F^- means that, like fluoride, the hydride anion would be expected to occupy the interior of a medium-size solvating cluster, whereas Cl^-, Br^-, and I^- prefer to remain at the surface [14–18]. This prediction was supported by our calculations and one question we were interested in was the optimum coordination number for solvated H^-. Heuft and Meijer [19] conducted a molecular dynamics simulation for solvated F^- and found the average coordination number to be 5 and the average dwell time of each solvating H_2O to be 16 ps. During their 20 ps simulation several H-bonds to fluoride formed and broke, maintaining the coordination of F^- between 4 and 6. Our 25 ps AIMD simulation of solvated hydride was done in part to look for similarities and differences between solvated hydride and fluoride.

We had four goals for the project. We wondered about the stability of small and medium-sized $(H^-)(H_2O)_n$ clusters, which we addressed by computing transition states. Second, we wanted to know how aspects of the cluster's topology (or H-bond connectivity pattern) could be enhance or impede reactivity, and whether any unifying principle(s) could explain the variety of reaction pathways. Third, we wondered low long the longest-lived hydrated hydride clusters might last. Lastly, through AIMD we explored how the finite cluster findings might translate to bulk liquid.

To approximate H^- in the context of bulk water we placed H^- inside a 5^{12} dodecahedral H_2O cage. Dodecahedral $(H_2O)_{20}$ has been much studied [20–23] because of its occurrence as a magic number [24–26] and its importance as a building block of von Stackelberg's Type I clathrate hydrate [27,28]. There is no experimental evidence for or against a dodecahedral geometry for $(H^-)(H_2O)_{20}$, but it is a plausible setup for a finite model of "hydride surrounded by water." The huge number of possible isomers meant we had to fix some parameters in order to obtain meaningful comparisons. In the dodecahedral $(H^-)(H_2O)_{20}$ several free H's point inward toward the anion. We postulated this could raise the cluster's transition energy barrier because as soon as the (H^-) approaches any one of the solvating donor H's and begins to react with it to form H_2, the result is suddenly a cage with several free H's pointing inward toward a neutral molecule, which is an energetically unfavorable arrangement. This prediction was borne out and probably represents our single biggest insight into the possible longevity of solvated hydride in bulk water.

2. Methods

Static *ab initio* calculations were done on a Parallel Quantum Solutions (PQS) QuantumCube, using PQS parallel software [29]. Relaxed PES scans for ground state electronic energy, denoted E^0, as a function of H^-– H distance, denoted d_{HH}, were the principal device for locating transition states. All reported transition states (also called "*t*-states") were first verified by a Hessian calculation. The *t*-state was then nudged slightly by adding or subtracting a small multiple of the "negative" eigenvector and gradient-following optimization was restarted using a small step size of 0.1 or less, to verify which local minima are reached going in both directions toward local minima. This is not identical with an intrinsic reaction coordinate (IRC) calculation [30–32], which would be the ideal method for determining a reaction pathway but is considerably more computation-intensive. For all but one of our pathways leading toward an $(H^-)(H_2O)_n$ geometry, there is no ambiguity about which isomer is the endpoint (the exception is discussed when we get to it). For pathways leading to $(H_2)(OH^-)(H_2O)_{n-1}$ geometries from *t*-states, a series of "choices" between competing rearrangements may need to be made about which way to proceed downhill, and the optimization method might sometimes make choices different from the IRC method. Therefore we do not claim that the $(H_2)(OH^-)(H_2O)_{n-1}$ isomers reported are always the exact isomers that would occur experimentally. Comparing and distinguishing among $(H_2)(OH^-)(H_2O)_{n-1}$ isomers might be an interesting subject but was not a focus of this project.

For all but the smallest clusters, B3LYP/6−311++G** was the method of choice to balance accuracy with computational tractability. In addition to its well-established use in water cluster studies in general, Swart [33] demonstrated the validity of DFT for H^+ affinity of solvated anions, and B3LYP/6−311++G** underwent further benchmarking against high-level MP2 for $(H^-)(H_2O)_n$ clusters by Lee et al. [8]. While DFT with a large basis is certainly a usable model for these systems, it does underestimate slightly the strength of a dihydrogen bond compared to MP2. Throughout this article, "B3LYP" will mean B3LYP/6−311++G** and "MP2" will mean MP2/aug-cc-pVTZ unless otherwise indicated. All reaction pathways we describe or show were computed with B3LYP except where they are specifically indicated to be MP2.

Ab initio molecular dynamics (AIMD) simulation applied the Vienna atomistic simulation package [34] (VASP) version 4.6, the Perdew–Burke–Ernzerhof (PBE) exchange correlation functional [35], and projected-augmented wave (PAW) pseudopotentials [36,37]. The default energy cutoffs for H and O were 400 eV. The cubic simulation cell contained one H^- anion and 32 H_2O molecules, and had edge length 9.8552 A, corresponding to a water density of 1.0 g/cc. A neutralizing charge background was added. A time step of 0.25 fs and an energy cutoff of 400 eV were adopted, and a Born–Oppenheimer convergence of 10^{-6} eV was enforced at each time step. These parameters limit the temperature drift to about 1 K/ps. A Nose thermostat was applied to maintain the temperature at $T = 300$ K. The deuterium mass was substituted for all protons to allow a larger time step, although the H mass is assumed whenever water density is reported. We continued the trajectory for 10^5 steps, representing 25 ps.

The initial AIMD configuration was prepared as follows. We started with the core $H^-(H_2O)_4$ of an optimized cluster, Dod-4A, to be described later. This core was held frozen while additional water molecules were added to yield a 1.0 g/cc density. These mobile water molecules were allowed to equilibrate at $T = 300$ K for 40 ps using classical force field-based molecular dynamics simulations. The final configuration thus generated was equilibrated using AIMD at $T = 300$ K for 2 ps before starting the collection of statistics for the next 25 ps.

3. Results: $2 \leqslant n \leqslant 6$

Table 1 summarizes all stationary states for $(H^-)(H_2O)_n$ clusters, $2 \leqslant n \leqslant 6$, that are mentioned in this article, along with their relative electronic energy (E^0) and relative free energy values (free energy at 0 K is computed as $G^0 = E^0 + ZPE$), dipole moments, and d_{HH} distances for the "index" or reacting proton.

3.1. n = 2

The single PES minimum geometry for $(H^-)(H_2O)_2$ was first described by Melin and Ortiz [38] as "Complex A". It has both waters solvating the hydride ion and one H-bond between the waters. The

Table 1
Dipole moment (Debye), B3LYP electronic energy and free energy (kcal/mol) at 0 K, and H–H⁻ distance (pm) for $(H^-)(H_2O)_n$ or $(H_2)(OH^-)(H_2O)_{n-1}$ stationary states, $2 \leqslant n \leqslant 6$.

n	Geometry	Dip	E^0	G^0	H	d_{HH}
2	h-2w	3.65	0.000	0.000	h1	144
	h-2w-ts	2.73	1.026	−1.022	h1	116
	h2ohw	2.61	−5.482	−7.252	h1	77
3	h-3wC3	2.72	1.346	1.684	h1	162
	h-3wC3-ts	2.58	2.504	1.844	h1	134
	h-3wCs-ts	2.94	2.250	0.891	h1	122
	h-3wCs	3.28	0.238	0.230	h1	142
	h-3wFLIP-ts	2.09	1.228	0.704	h1	141
	h-3wC2	0.30	0.000	0.000	h1	142
	h-3wC2-ts	3.47	2.570	0.176	h1	110
	h2oh-w2A	3.80	−9.077	−12.122	h1	75
4	h-4wB	1.20	0.000	0.000	h1	146
	h-4wB-ts	2.15	1.397	−0.524	h1	105
	h2oh-w3B	4.43	−12.357	−14.478	h1	75
4	h-4wCs	1.09	0.000	0.000	h1	147
	h-4wCs-ts	2.54	2.631	−0.180	h1	104
	h2oh-w3A	3.52	−10.012	−14.619	h1	75
5	h-5wA	3.18	0.004	0.049	h3	137
	h-5wA-ts[h3]	2.53	0.663	−1.133	h3	113
	h2oh-4wA[h3]	4.11	−14.127	−16.651	h3	75
	h-5wA-ts[h2]	1.22	4.291	1.305	h2	98
	h2oh-4wA[h2]	3.13	−11.189	−15.402	h2	75
	h-5w-F8-ts	3.78	1.136	0.513	h1	141
	h-5wE	4.14	0.991	0.639	h1	143
	h-5w-F6-ts	3.97	1.250	0.777	h1	142
	h-5wD	3.14	0.000	0.000	h1	140
	h-5w-SD-ts	3.49	1.244	0.419	h1	143
	h-5wD-ts	2.54	0.768	−0.958	h1	112
	h2oh-w4D	3.55	−14.375	−17.212	h1	75
6	h-6wC2	1.82	0.000	0.000	h1	150
	h-6w-LH-ts	2.83	0.810	0.190	h1	141
	h-6wB	4.18	−0.744	−1.088	h1	132
	h-6wB-ts	2.89	0.219	−1.883	h1	105
	h2oh-5wB	4.92	−13.948	−16.474	h1	75
6	h-6wD	2.10	0.000	0.000	h1	133
	h-6wD-ts	2.05	1.296	−0.767	h1	101
	h2oh-5wD	4.30	−14.753	−17.668	h1	75

reaction pathway involves breaking the water–water H-bond at the same time as the nearer solvating H approaches the hydride. At the transition state, d_{HH} is 116.1 pm (111.4 pm by MP2). The transition energy barrier ΔE^0 is 1.03 kcal/mol (0.84 kcal/mol by MP2), but the ZPE correction of –2.05 kcal/mol (–1.85 by MP2) overwhelms this barrier, making ΔG^{ts} negative (–1.02 kcal/mol by B3LYP, –1.01 kcal/mol by MP2).

A PES where harmonically-computed ZPE corrections place a transition state below one of the minima it connects ($E^0(ts) > E^0$(Min#1) while $G^0(ts) < G^0$(Min#1)) can be tricky to interpret. If the calculated ZPE is close to being accurate, it means there is no separate bound quantum state for Min#1. One must be careful because a shallow PES minimum will also be a minimum where the harmonic approximation may apply poorly, so the true ZPE correction can be smaller and Min#1 might have a bound quantum state. However, on the $H_5O_2^-$ PES, Min#2 (h2ohw) sits quite far below Min#1 (h-2w) at –5.5 kcal/mol (Table 1), and if there is a bound state for h-2w the barrier would be <1 kcal/mol. Hydride (one proton mass) could probably tunnel across a barrier under 1 kcal/mol, and on this basis we predict that h-2w is unstable or barely stable.

3.2. n = 3, and figure conventions

Three local minima have been identified for $(H^-)(H_2O)_3$ [39]. They have symmetry groups C2, C3, and Cs and we denote them as h-3wC2, h-3wC3, and h-3wCs, respectively. The h-3wC2 geometry is the global minimum, with h-3wC3 almost isoenergetic. The geometries h-3C2 and h-3Cs interconvert by flipping the orientation of the free H on either of the solvating H_2O's. These H_2O's are of the 'DA' type (single donor single acceptor) and clusters that contain DA water molecules typically have more than one stable orientation for the free H (*cf.* studies by Wales and others of up-down flips for the free H's in the water tetramer [40–42]). Flipping of a free H on a DA occurs in neutral water clusters and has been studied by tunneling spectroscopy for the cyclic water trimer through pentamer [43–47]. As with $(H_2O)_3$ to $(H_2O)_5$, the energetic barrier for flipping from 3Cs and 3C2 is low: it is 0.99 kcal/mol, and 0.47 kcal/mol when ZPE correction is included (resp. 0.94 and 0.54 by MP2).

The three $(H^-)(H_2O)_3$ geometries, along with transition states and a final reacted geometry, are illustrated in Fig. 1. The names we give to the various isomers are listed below their drawings. The curve gives E^0 as a function of a reaction coordinate, while the horizontal line segments show the relative values of G at 0 K for the various stationary states, where $G = E^0 + \text{ZPE}$. (A vertical offset is added to all G values in a figure to help them fit more nicely on the graph, so for each figure their positions differ by a fixed amount from the values given in Table 1.) In Fig. 1, as in all our figures, blue is hydride and red is O. 'Yellow' is generally reserved for the index proton that is reacting with the hydride, so that the yellow–blue separation is d_{HH}.

Other colors denote other water H's. Color identifies protons in a consistent manner for all isomers shown in a single figure. Specific atoms and their bonds can be tracked visually from isomer to isomer by following the colors. Individual atoms are also given names, but to avoid crowding the drawings with labels we make the labels "implicit" via the following convention. For one $(H^-)(H_2O)_n$ cluster in each figure, the O atoms are labeled 1 through n and called o1, o2, ..., (o)n, and this labeling implicitly transfers to all the other isomers in that figure. The corresponding H_2O units will be called w1, w2, ..., (w)n. The H's of water unit (w)i are called (h)i and (h)$n + i$. To decide which proton is which, if one of them is in a dihydrogen bond it is automatically (h)i and the other one is (h)$n + i$, but for H_2O's not adjacent to H^-, (h)i is identified in one drawing if we need to refer to it. For example, using the labels on h-3wC3 in Fig. 1, the convention means that throughout Fig. 1 ($n = 3$), the yellow proton is h1, the green proton is h4, gray is h2, white is h5, bronze is h3, and orange is h6. The hydride H (blue) is always given the special name h0. If the index proton is not otherwise labeled, it is given the name 'h1' in Table 1.

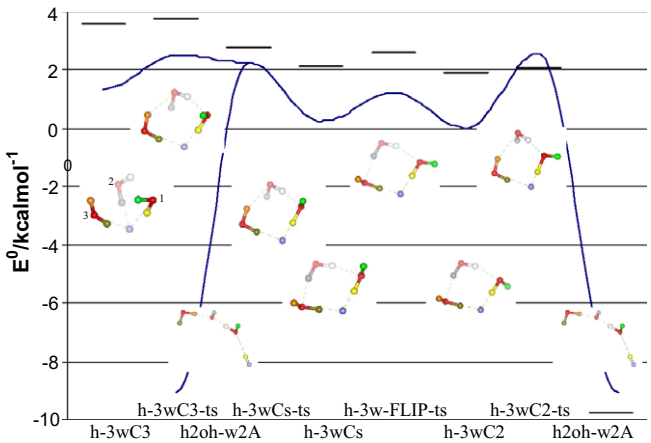

Fig. 1. Stationary states, electronic energies, and relative free energies for $(H^-)(H_2O)_3$.

Returning to $(H^-)(H_2O)_3$, if either solvating proton in h-3wC2 is brought toward the H^-, a *t*-state is found beyond which the cluster undergoes reaction and reorganization as $(H_2)(OH^-)(H_2O)_2$, as illustrated on the right-hand side in Fig. 1. We denote the *t*-state as h-3wC2-ts and the final geometry as h2oh-w2A. The same holds for h-3wCs (*t*-state is called h-3wCs-ts). To describe the reaction pathway, follow h2 and h6, i.e. the gray and orange protons, and their O's o2 and o3 on water molecules called w2 and w3. In going from h-3wC2 to h-3wC2-ts, w3 rotates around the o3—H^- (or o3–h0) bond while w2 rotates in the opposite direction, like gears. Oxygens o2 and o3 remain H-bonded but h6 has replaced h2 as the bonding proton and the H-bond direction has reversed. A similar "gear rotation" characterizes how h-3wCs-ts derives from h-3wCs. Its activation barrier is $\Delta G^{ts} = 0.66$ kcal/mol compared to $\Delta G^{ts} = 0.18$ for h-3wC2-ts. Thus the reaction pathway for h-3wCs with lowest Gibbs energy barrier is to first "detour" via a flip to h-3wC2 (barrier 0.47), and then to crest h-3wC2-ts (barrier 0.18). The reacted geometry going directly downhill from h-3wCs-ts happens to converge to the same isomer h2oh-w2A.

We located a transition state, denoted h-3wC3-ts, which when nudged in one direction falls back to h-3wC3. In the other direction optimization converged to h-3wCs-ts. This is the unique situation, referred to above, where the optimization method may mislead. If the same result were found using IRC it would mean this is an example, or is very close to being an example, of an uncommon phenomenon called a valley-ridge inflection (VRI). A VRI is a PES feature where, after crossing a *t*-state, the intrinsic reaction pathway descends to a *t*-state between two other minima [48]. Fig. 1 shows the ambiguity as a branching pathway, indicating our method did not determine which direction would be followed. With ZPE correction, h-3wC3-ts sits just 0.16 kcal/mol higher than h-3wC3, making h-3wC3 barely stable or unstable. The VRI-like feature was not seen via MP2: instead, MP2 found a single *t*-state connecting h-3wC3 and h2oh-w2A, of barrier height $\Delta E^0 = 1.83$, which became –0.77 kcal/mol with MP2-calculated ZPE correction.

3.3. n = 4

Many PES local minima exist for $(H^-)(H_2O)_4$ [8]. The global minimum (by MP2) has Cs symmetry, denoted here as h-4wCs (*cf.* Fig. 2), and its nearly isoenergetic runner-up, here denoted h-4wB, is constructed by adding another H_2O, called w4, at the hydride of h-3wC2 (*cf.* Fig. 3) [39]. For h-4wCs, the *t*-states for H^- approaching either of the nearer H_2O's are the same, and we denote the *t*-state for H^- approaching h1 (yellow in Fig. 2) and its oxygen (o1) as h-4wCs-ts. Along the reaction pathway, the H-bond from o2 to o3 breaks, making h2 (gray) non-H-bonded, and h7

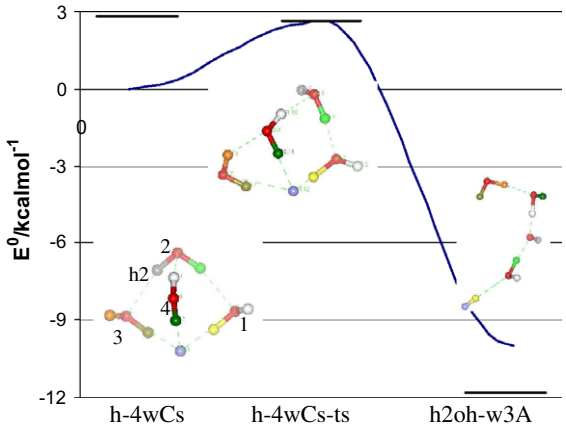

Fig. 2. h-4wCs geometry, transition state, and product.

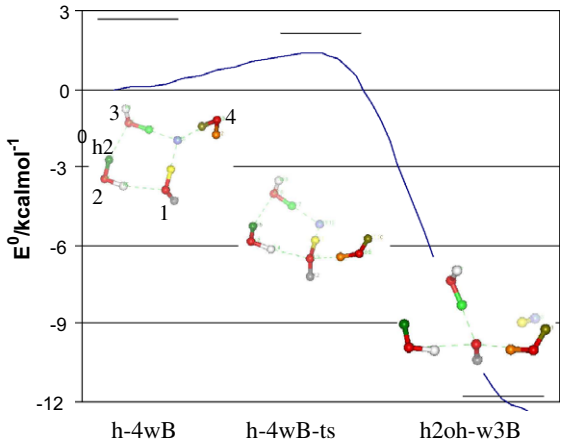

Fig. 3. h-4wB geometry, transition state, and product.

(orange) forms a new H-bond between o3 and o4. At the *t*-state $d_{HH} = 104.0$ pm and $\Delta E^0 = 2.62$ kcal/mol, but with ZPE correction this becomes negative, $\Delta G^{ts} = -0.19$, indicating quantum instability. To reach the final configuration, h2oh-w3A, the dihydrogen bonds of o3 and o4 break, and h1 and h6 (yellow and green) undergo proton transfer.

The *t*-state for h-4wB, denoted h-4wB-ts, is shown in Fig. 3. In going from h-4wB to h-4wB-ts, h4 (bronze) detaches from the hydride and h8 (orange) forms a new H-bond with the emerging OH^- at o1. The *t*-state has $d_{HH} = 104.6$ pm, $\Delta E^0 = 1.39$ kcal/mol, and $\Delta G^{ts} = -0.53$, so h-4wB is unstable. For the final $(H_2)(OH^-)(H_2O)_3$ configuration, denoted h2oh-w3B, h1 completes its transfer and h3 switches its H-bond from h0 to the new OH^- at o1.

3.4. n = 5

For the case $n = 5$ we put a special emphasis on understanding how and why pathways differ for the three solvating protons. Lee et al. [8] described a single global minimum $(H^-)(H_2O)_5$, called 5Y32 there and h-5wA here. It has a triangular prism shape and is shown as Fig. 4(h). Closely related to h-5wA are two other local minimum configurations: h-5wE, obtained by flipping h8 (green) and shown as Fig. 4(c); and h-5wD, obtained by also flipping h6 (bronze), shown as Fig. 4(a). By B3LYP, h-5wD is isoenergetic with h-5wA: E^0 favors h-5wD over h-5wA by just 5 cal/mol, and their ZPE's differ by 45 cal/mol (*cf.* Table 1). The transition states for the flips, h-5w-F8-ts and h-5w-F6-ts, are shown as Fig. 4g and b, respectively.

An alternate *t*-state, shown as Fig. 4d, connects h-5wE with another configuration, Fig. 4e. In going from Fig. 4c to 4e, w4 (the H_2O with two gray protons) detaches from the H-bond in which it is the acceptor (of h2), and swings like a door on hinges to become instead acceptor of a new H-bond with h1. The "hinges" are the oxygens o5 and o3, which stay approximately fixed during the move. The H-bonds connecting o4 to o5 and to o3 remain intact during the move and define the plane of the "door". "Swinging door" is the source of our name h-5wSD-ts for Fig. 4d. If the final configuration Fig. 4e is rotated 120° to the left as in Fig. 4f, it is seen to be the mirror image of Fig. 4h, h-5wA. Thus two *t*-states connect h-5wE with h-5wA, but if one were to traverse the loop in Fig. 4, the cluster would undergo reflection and waters w1 and w2 would exchange places. This could be experimentally relevant if some of the O's or H's were replaced by isotopes.

Given this understanding of Fig. 4, let us consider Fig. 5. The motivation for Fig. 5 was to explore how each of h1, h2, h3 in h-5wA would react to form H_2. On the left side of Fig. 5, h1 of h-

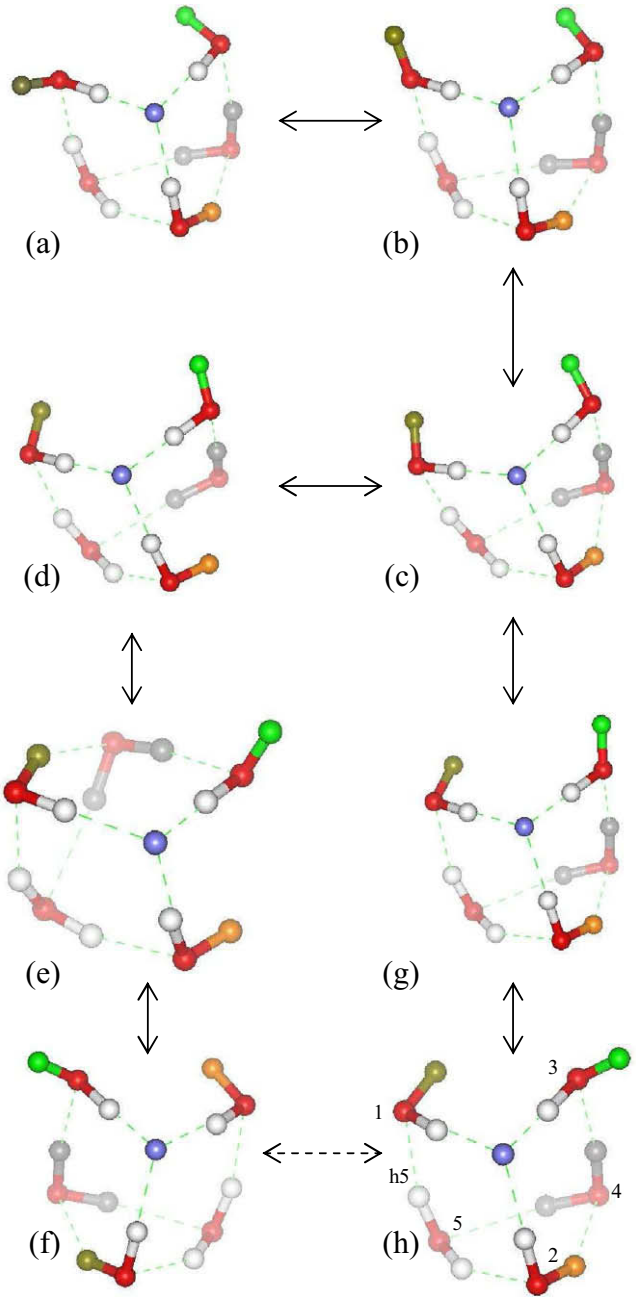

Fig. 4. $(H^-)(H_2O)_5$ stationary states. (a) h-5wD; (b) h-5w-F6-ts; (c) h-5wE; (d) h-5wSD-ts; (e) h-5wA; (f) h-5wA; (g) h-5w-F8-ts; and (h) h-5wA.

5wD reacts with h0, and the *t*-state h-5wD-ts has d_{HH} = 112.3 and ΔG^{ts} = –0.96, verifying the instability of h-5wD. The only topology change in going from h-5wD to h-5wD-ts is that the h8—o1 distance shortens from 292.9 to 195.2. Moving to the right from h-5wD we have the same sequence of isomers as Fig. 4a–e. Drawings of h-5wF6-ts and h-5wSD-ts are omitted from Fig. 5 for space reasons and their names are placed in brackets to indicate "not depicted", but their E^0 and G^0 values are included in Fig. 5. The reaction of h1 of h-5wA with h0 would occur by following the 3-step pathway of Fig. 5, i.e. via h-5wSD-ts to h-5wE, then via h-5wF6 to h-5w-D, and then via h-5wD-ts to h2oh-4wD. The maximum free energy along the 3-step pathway would be ΔG^{ts} = 0.72 (relative to h-5wA) at h-5w-F6-ts. Proton h2 (dark green) of h-5wA can react via the *t*-state h-5wA-ts[h2], which is obtained from h-5wA by another swinging door move in which w1 ceases to be

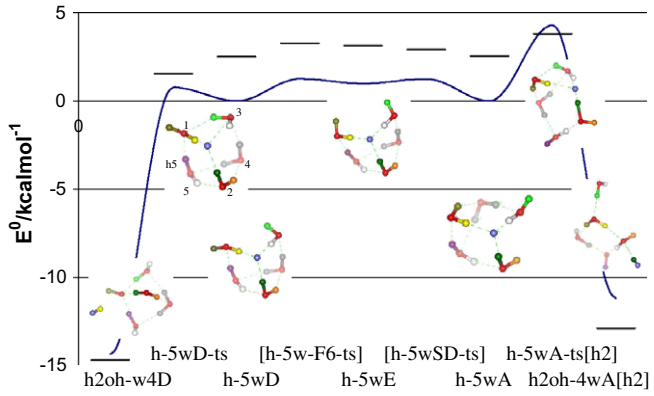

Fig. 5. Selected stationary states, electronic energies, and relative free energies for $(H^-)(H_2O)_5$.

acceptor of h5 and becomes acceptor of h8. At this *t*-state, d_{HH} (i.e. the h2—h0 distance) is 98.2 pm, ΔE^0 = 4.27 kcal/mol, and ΔG^{ts} = 1.24 kcal/mol. Lastly, we do not illustrate the reaction of h3 with h0 for h-5wA because it is just like the reaction of h1 for h-5wD. The principal change in forming h-5wA-ts[h3] is that the h7—o3 distance drops from 259.5 in h-5wA to 195.2. It has d_{HH} = 112.9 pm and ΔG^{ts} = –1.18 kcal/mol.

3.5. n = 6

Ref. [39] recognizes two nearly isoenergetic minima for $(H^-)(H_2O)_6$, one having coordination 4 at the H^- and C2 symmetry (called here h-6wC2) and the other having a prism shape with coordination 3 and C1 symmetry (called here h-6wD). For h-6wD, the *t*-state for H^- approaching the nearest H_2O, denoted h-6wD-ts, has the same topology as h-6wD with d_{HH} = 100.7 pm, ΔE^0 = 1.30 kcal/mol, and ΔG^{ts} = –0.77. For h-6wC2, Fig. 6 illustrates that the reaction is a two-step process. In step 1, one solvating H_2O, w3, commits a Laage–Hynes move [49] to create a variant of h-6wD, denoted h-6wB. In the *t*-state for this Laage–Hynes move, called h-6w-LH-ts, h3 (bronze) is switching its acceptor from the H^- (h0) to the target oxygen (o1), and the h3—h0 and h3—o1 distances are 295.3 and 318.4 respectively. For this transition, ΔE^0 = 0.81 kcal/mol, and ΔG^{ts} = 0.19. In the second step, the hydride combines with h1 (yellow). The *t*-state h-6wB-ts is similar to h-6wD-ts, with d_{HH} = 104.6 pm, ΔE^0 = 0.96 kcal/mol, and ΔG^{ts} = –0.80. Because the h-6wD pathway is so similar to that of h-6wB, i.e. the second step in Fig. 6, the h-6wD pathway is not separately illustrated. The negative ΔG^{ts} values show that h-6wD and h-6wB are probably unstable at 0 K, and h-6wC2 is unstable or barely stable.

3.6. Preliminary dihydrogen bond length analysis

A quick glance at the dihydrogen bond lengths among the optimized local minimum clusters gave a range of 132–191 pm, with

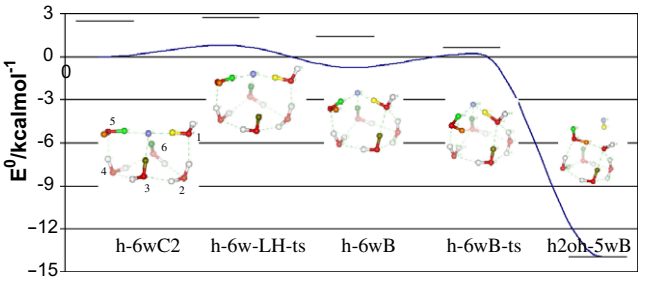

Fig. 6. Selected stationary states, electronic energies, and relative free energies for $(H^-)(H_2O)_6$.

the shortest H–H⁻ distances occurring when the donor H is on a DAA and the longest distances occurring when the donor H is on a DD. To verify that this pattern was genuine, we treated all our H–H⁻ distances as a dataset and correlated them with donor type (i.e. the type of the O of the donor H). Because the coordination number of the hydride also affected H–H⁻ distances, with longer distances at higher coordination numbers, we focused just on clusters where the hydride coordination was 3. We had 48 H–H⁻ bonds in optimized clusters whose hydride coordination was 3. The majority of these clusters were obtained while searching for low-energy structures and were not included in the above results. We do not claim that they are representative or random in any particular way. Still, we regressed d_{HH} against D–A, where "D–A" is obtained by subtracting the number of H-bonds in which the donor's O is an acceptor from the number in which it is a donor. This gave the formula

$$d_{HH} \approx 146.4 + 16.4(D - A) \quad (2)$$

The RMS error was 5.4 pm and r^2 was 0.84, i.e. this simple formula accounts for 84% of the variance among H–H⁻ distances. There were several instances where the value of 'D' or 'A' was ambiguous because the O was involved in a very weak H-bond with R_{HO} between 2.3 and 2.7 Å. It improved the formula's performance if these weak bonds were included as if they were worth 1/3 of a regular donor or acceptor: RMS error improved to 5.0 and r^2 improved to 0.87. There was a slight improvement from introducing separate parameters of 'D' and 'A' but this was not statistically significant ($p > 0.08$). p-Value for the coefficient in (2) to be nonzero was $<10^{-6}$.

4. Discussion: $2 \leqslant n \leqslant 6$

We have identified four principal patterns of topology realignment that small $(H^-)(H_2O)_n$ clusters undergo along their reaction pathways to a transition state: bond breakage/formation, gear flip, Laage–Hynes move, and swinging door. Each of these was observed in at least two clusters. We have de-emphasized the rearrangements that occur between the t-state and the $(H_2)(OH^-)(H_2O)_{n-1}$ geometry, but these mostly featured H-bond breakage/formation and proton transfers that shift the location of the OH^-. In $(H_2)(OH^-)(H_2O)_{n-1}$ clusters the H_2 always chooses an orientation in which H—H—O is nearly collinear, the 'O' being either the O of OH^- or an O adjacent to the OH^-. Free energy barriers for formation of H_2 at 0 K (ΔG^{ts}) range from −1.18 to 1.24 kcal/mol, and d_{HH} at these t-states ranges from 122.3 to 98.2 pm.

Considering the set of H_2-forming t-states as a whole (i.e. omitting flips or others between two solvated hydride states), there is generally speaking a positive association between having less rearrangement and having a lower barrier. There is a slight trend for the value of d_{HH} at the t-state to go down as n increases, probably because of higher coordination of the hydride initially.

Is there any underlying principle that unifies the wide variety of rearrangements that occur along reaction pathways? The explanation begins with Formula (2). The formula can be understood as revealing a solvation preference hierarchy, i.e. the strength of an H_2O solvating a hydride varies with the type of the H_2O according to the series

$$DAA > DDAA \approx DA > DDA \approx D > DD \quad (3)$$

Series (3) also describes decreasing bond strength (and increasing bond length) as a function of donor's type for H-bonds in water clusters in general. However, when an anion is present, the energy gained by moving up the hierarchy for solvators of the anion will be much greater than for solvators of other H_2O's or of other neutral H-bond acceptors. Hence the number and types of the solvators of the anion are the dominant factor determining the energetic favorability of a small water–anion cluster. When the anion is OH^-, an additional consideration is that the H of OH^- makes a poor H-bond donor, so this H "prefers" to be non-H-bonded. This simple principle of "anion solvation preference" is the key to understanding the changes that occur along all our reaction pathways.

As d_{HH} decreases along the reaction pathway, negative charge gradually shifts away from the H^- and onto the emerging OH^- at the O that initially holds the reacting proton. Therefore the system is gradually shifting from one whose energetic considerations are dominated by the solvation hierarchy (3) applied to the hydride, to a system whose energetic considerations are dominated by the solvation of the hydroxide. In every instance we studied, *the specific rearrangements that occur along the reaction pathway can be understood as the system's way of adjusting so as to optimize solvation of the moving negative charge* in better accord with the solvation hierarchy (3). For example, in h-3C2, h0 has two DA solvators and o1 has a DD solvator. After gear flip, h0 has the DD and o1 is solvated by a DA. The Laage–Hynes move in Fig. 6 reduces the solvation number (coordination) of h0 and increases solvation of o1. In Fig. 5, the 3-step pathway for h1 of h-5wA involves first making h6 non-h-bonded by the swinging door move, and ultimately adding h8 as a second solvator at o1. Reaction pathways have the lowest barriers and involve little or no rearrangement, when the initial geometry starts out favorable for the target O to become OH^-. An example of this is h-6wB of Fig. 6, where o1 starts out as a DAA (i.e. h7 is non-h-bonded and o1 has two solvating H_2O's).

We are reminded of Tuckerman's concept of "presolvation", the principle that proton transfer occurs in water containing H_3O^+ or OH^- only after the neighboring H_2O's become favorably configured for the shift [50,51]. Local rearrangements drive proton transfer events, not the other way around. Likewise, the barrier for transfer of a proton to hydride depends on presolvation of the donating O, i.e. the suitability of its solvation shell to support becoming OH^-.

All of the clusters for $2 \leqslant n \leqslant 6$ are unstable or barely stable because one pathway or another is relatively favorable. Is there any way to design a hydride-water cluster so that all pathways are relatively unfavorable? This is one question that we pursued in the next section. Armed with the insights provided by these smaller systems, we deliberately tried to see whether an $(H^-)(H_2O)_n$ could be designed that would be exceptionally long-lived. If so, a small fraction of solvated hydrides in liquid water might adopt this form and achieve a detectable steady-state population of aqueous H^-.

5. Results and discussion: $n = 20$ and AIMD

5.1. Selection of clusters

We optimized a variety of $(H^-)(H_2O)_{20}$ clusters consisting of a hydride anion encapsulated by a 5^{12} dodecahedral cage, using B3LYP. If c denotes the coordination number of the hydride, then c protons that would be free ("dangling") for the empty cage must be inverted to point inward toward the hydride. Parameters that can affect cluster energy and geometry include the choice of which water molecules of the cage should donate the c solvating protons, the positions of the $10–c$ remaining (outward-pointing) free protons, and the directions of the 30 inter-water hydrogen bonds. Given that the energy of empty dodecahedral cages has a range of some 30 kcal/mol [21], we anticipated that the same might be true of hydride-encapsulating dodecahedra. Finding the global minimum-energy $(H^-)(H_2O)_{20}$ cluster was not our focus, but we wanted examples that had at least relatively low energy. Low energy clusters would be most representative of what might occur for a solvated hydride in bulk water, and this is what would occur if $(H^-)(H_2O)_{20}$ were made in an experimental system.

For empty dodecahedral cages, E^0 has a strong positive correlation with the number of "defects", a term introduced by Smith and Dang [52] to refer to the number of adjacent free protons on the surface, i.e. the number of DAA–DAA H-bonds. Let 'b_0' denote the number of DAA–DAA bonds. For (empty) dodecahedral clusters and for polyhedral water clusters (PWCs) in general this number always coincides with the number of DDA–DDA bonds, so it was not automatically clear from PWC studies whether the increase in E^0 that came with more defects was due to the DAA–DAA bonds, to the DDA–DDA bonds, or both. The fact that the lowest-energy 11-mer inserts a DA into the DAA–DAA bond of the pentagonal prism rather than into the DDA–DDA bond or anywhere else [53] suggests that breaking up DAA–DAA bonds matters most to lowering E^0. Empty 5^{12} dodecahedra must have at least 3 DAA–DAA bonds [54,55], i.e. $b_0 \geqslant 3$, but $(H^-)(H_2O)_{20}$ clusters can have $b_0 = 0$ if one of the DAA's in each DAA–DAA bond is among the H_2O's whose dangling H's are inverted (so that they H-bond to the H^- and become DDAA). In optimizing $(H^-)(H_2O)_{20}$ clusters we observed that those with $b_0 > 0$ have higher electronic energy than otherwise similar clusters having $b_0 = 0$, by 2 kcal/mol or more. The effect of the number of DDA–DDA bonds on E^0 is small by comparison. This observation served both as a confirmation that DAA–DAA bonds are the principal origin of the energy-defect correlation for PWCs, and as a guide to focus our attention on $(H^-)(H_2O)_{20}$ clusters having no DAA–DAA bonds. For empty 5^{12} cages, Singer and coworkers [21] found that increasing b_0 by 1 adds about 4 kcal/mol to E^0.

Concerning the choice of dangling OH's to invert, it makes intuitive sense that enhanced stability would come with keeping the c solvator protons as far apart as possible. When $c = 4$ there is a "natural" way to do this by choosing the solvators to lie at the corners of a regular tetrahedron, every pair being separated by 3 H-bonds, and for $c = 3$ the optimum is to let them lie along an equator (so their separations are 3, 3, and 4 H-bonds). The 5^{12} with a tetrahedrally coordinated central H_2O is the structure suggested by Shin et al. [26] for the magic number $(H^+)(H_2O)_{21}$. For $c = 5$ we used an arrangement that approximates the double tripyramid. For $c = 6$, the octahedral setup commonly found for 6-coordinated species does not align well with the discrete positions available in the 5^{12} cage, and we used the closest sites. It is possible that a cage other than 5^{12} would be preferred for a six-coordinated $(H^-)(H_2O)_{20}$ cluster.

We considered 16 symmetry-distinct configurations obeying the three combined conditions of $c = 4$, tetrahedrally placed solvators, and $b_0 = 0$. Lacking a better word we call these "ideal" configurations. We optimized all 16 and chose the cluster with lowest-energy (called h-dod4A) and also took one whose energy fell in the middle of the list (called h-dod4B) for further exploration. For $c = 3, 5, 6$, we optimized several $(H^-)(H_2O)_{20}$ clusters having $b_0 = 0$ and with solvator placement as described above. All of these had notably higher E^0 and higher E^0 + ZPE than any of the 16 ideal structures. We did not conduct an extended search for the global c-coordinated minimum for $c = 3$, 5, or 6, but merely selected the lowest-energy cluster among those we examined for each c value, for reaction studies. These are denoted h-dod3A, h-dod5A, and h-dod6A, and are illustrated in Fig. 7, along with h-dod4B. For the h-dod4A cluster see Fig. 8. Table 2 lists E^0 and $G^0 = E^0$ + ZPE for each structure, with E^0 and G^0 for h-dod4A taken as "zero." The labels w1, ..., (w)c were assigned to the hydride-solvating waters in increasing order of d_{HH}, i.e. h1 is the closest H to h0, h2 is the next closest, and so on. Clusters h-dod4A and h-dod5A appear more than once in Table 2 as a way of listing their H–H^- separations for different solvating protons, since pathways for multiple protons are explored.

5.2. Simple reaction pathways

By starting at one of the dodecahedral minima and focusing on one solvating H and conducting a series of constrained optimizations with d_{HH} for that H fixed at various values, we could generate a one-variable relaxed PES curve. Along these E^0-vs-d_{HH} curves, two patterns are noted. In one pattern, a smooth curve is found and the original topology is preserved up to a maximum E^0 and generally for a little distance beyond it. In these cases the maximum occurs between 95 and 81 pm, and always turns out to be a *bone fide* transition state. In the other pattern, a single Laage–Hynes move switches one solvating proton from h0 to the target O before a maximum is reached, but after that one rearrangement, the E^0-vs-d_{HH} curve continues smoothly over a maximum which is a verifiably a transition state. We call these pathways "simple" since inching one proton toward the hydride is the "obvious" way to look for a t-state, and the pathways found this way involves only what rearrangements are absolutely necessary to get to a t-state.

A "full calculation" for a simple pathway consisted of a segment of the E^0-vs-d_{HH} curve to check for spontaneous rearrangements, t-state optimization starting near the curve's maximum, FREQ check for the t-state, verification that optimization from a "nudge" of the t-state regenerates the starting geometry, and computation of the product configuration, i.e. the final $(H_2)(OH^-)(H_2O)_{19}$. The full calculation was done for all four solvator protons of h-dod4A, and for the h1 proton in h-dod3A, h-dod4B, and h-dod6A. For h-dod5A, we computed enough of the curve near the transition state for all five protons to see what the patterns are, and determined in the process that the simple pathway for h2 has the lowest activation barrier and for h1 the highest. The full calculation was then done for h2 and h1 of h-dod5A. In all, 9 protons got the full calculation and for h3, h4, and h5 of h-dod5A we determined the simple pathway pattern.

The first pattern occurred for the solvating protons of the 3- and 4-coordinated dodecahedral clusters and for proton h1 of h-dod5A. The second pattern occurred in all other cases. When the second pattern occurs, the H_2O that does the Laage–Hynes move has its O located two H-bonds away from the target O. The first pattern occurs when the target O is situated 3 H-bonds or more from all the other hydride-solvating waters. An H_2O that is three H-bonds away has to "reach" much further to enact a Laage–Hynes move compared to one that is just two H-bonds removed. The distinction between the first and second pattern seems to be a simple matter of whether a properly situated solvating H is available to do Laage–Hynes, though the higher coordination number (5 or 6 vs. 3 or 4) probably also plays a role in "driving" the move.

Fig. 7 also shows the t-states and product geometries of the simple pathway, for the h1 protons of h-dod3A, h-dod4B, and h-dod6A, and for h2 of h-dod5A. For the latter two, where the second pattern applies, notice that the Laage–Hynes protons (h5 for h-dod5A and h6 for h-dod6A) donate to the index O at their transition states, making this O a triple acceptor. When h-dod6A-ts is nudged and optimized, h-dod6A is recovered, which means that from h-dod6A to h-dod6A-ts the reaction proceeds without intermediates, but this is not true of h-dod5A-ts. Instead there is a new local minimum, denoted h-dod5A-LH, where h5 remains H-bonded to o2 and h0 is only 4-coordinated. The reaction pathway must cross a t-state between h-dod5A and h-dod5A-LH, called h-dod5A-LH-ts, at which h5—o2 = 235.7 pm and h5—h0 = 286.9 pm. (This transition is similar to h-6w-LH-ts.) However, with ZPE correction h-dod5A-LH-ts has lower free energy at 0 K than h-dod5A-LH, so the latter is unstable and converts barrierlessly to h-dod5A.

All of these geometries are summarized in Table 2. As Table 2 shows, reaction of h1 of h-dod4B occurs at a significantly lower ΔG^{ts} and at a higher value of d_{HH}, compared to any of the simple pathways for h-dod4A. The reason is that o1 of h-dod4B is the acceptor in an H-bond with a DAA (the bonding proton is h5), whereas all four hydride-solvating H_2O's of h-dod4A only accept

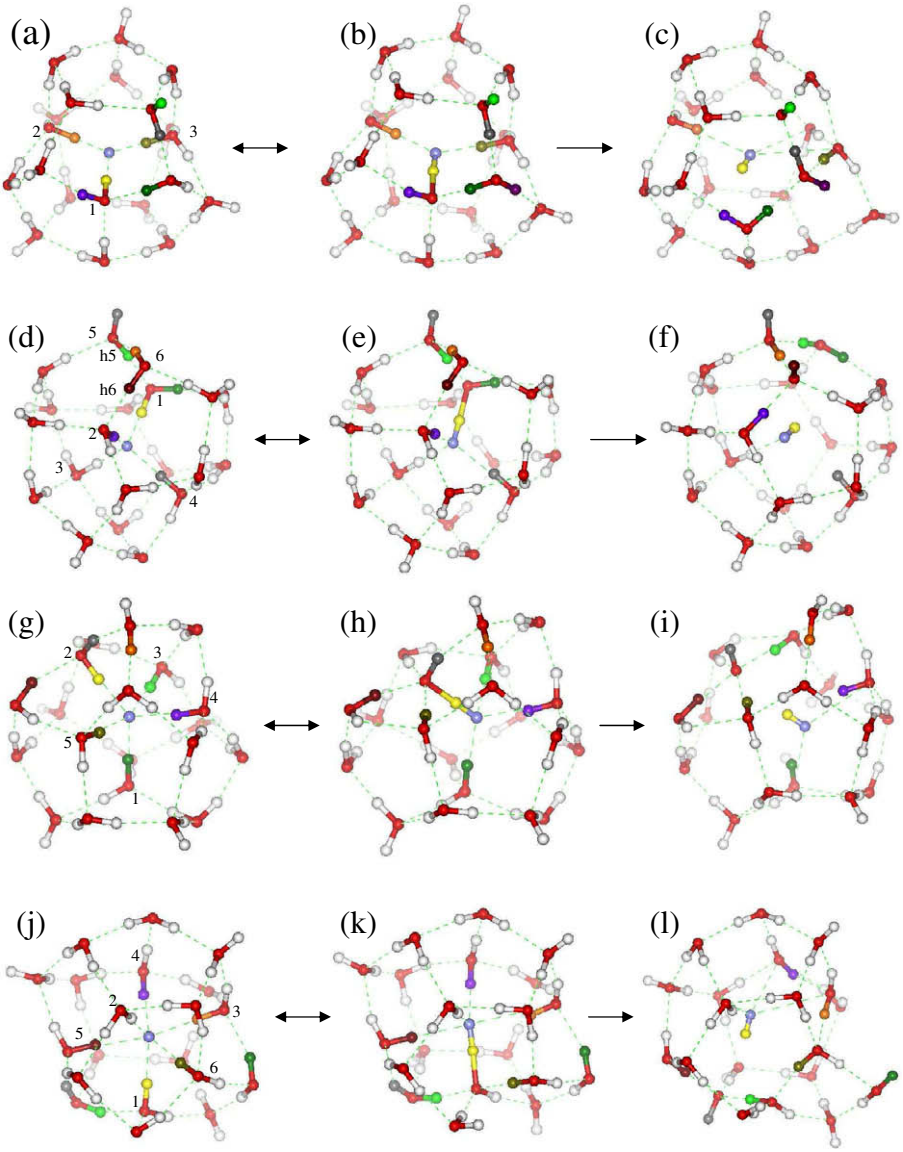

Fig. 7. $(H^-)(H_2O)_{20}$ stationary states: encapsulated hydride, transition state of simple pathway, and $(H_2)(OH^-)(H_2O)_{19}$ product, for four initial configurations. (a) h-dod3A; (b) h-dod3A-ts; (c) h2oh-w19-3A; (d) h-dod4B; (e) h-dod4B-ts; (f) h2oh-w19-4B; (g) h-dod5A; (h) h-dod5A-ts; (i) h2oh-w19-5A; (j) h-dod6A; (k) h-dod6A-ts; and (l) h2oh-w19-6A.

H-bonds from DDA's. As indicated in the hierarchy (2), DAA is a better solvator of OH^- than DDA, so o1 of h-dod-4B is better presolvated to become OH^- than any O of h-dod4A. Notice that proton h5 ends up transferred to o1 in the final configuration, h2oh-w19-4B (Fig. 7(f)). One interesting feature of the pathway from h-dod4B-ts to h2oh-w19-4B is that it contains a gear flip in which h2 replaces h6 to reverse the direction of the o2—o6 H-bond.

5.3. Another pathway for h-dod4A

Given the large size of the clusters and the plethora of conceivable pathways, exploration of possible reaction routes other than the simple pathways for $(H^-)(H_2O)_{20}$ is quite a complicated undertaking. We attempted this only for our lowest-energy cluster, h-dod4A. We reasoned that a lower-barrier pathway would have to improve presolvation for the target O, which means the system would first undergo some kind of H-bond rearrangement on the cage surface. However, any H-bond rearrangement has its own energetic barrier, and most have barriers exceeding the 5 kcal/mol threshold that the simple pathways offer.

We did find one pathway whose barrier height is lower than 5 kcal/mol, for the proton h3. This pathway is illustrated in Fig. 8. It involves breaking the o6—o5 H-bond and re-making it in the reverse direction. Oxygens o6 and o5 start out as DAA and DDA respectively but end up as DDA and DAA. There is an intermediate local minimum geometry in which there is no H-bond and both are DA. After the switch, the cluster is no longer one of the "ideal" set and we denote it h-dod4Z. The H-bond from o5 to o3 is not affected, and therefore this move turns o3 into an acceptor from a DAA (which makes it better presolvated). The intermediate with two DA's is called h-dod4X and is shown in Fig. 8. The *t*-states from h-dod4A to h-dod4X, denoted h-dod4X-F5-ts, and from h-dod4X to h-dod4Z, denoted h-dod4X-F6-ts, are like the *t*-states for free H flips, and are not depicted. Thus the pathway starting at h-dod4A traverses three *t*-states: via h-dod4X-F5-ts to h-dod4X, then via h-dod4X-F6-ts to h-dod4Z, and finally via the H_2-forming h-dod4Z-ts to a final h2oh-w19-4Z. At low temperatures the rate-

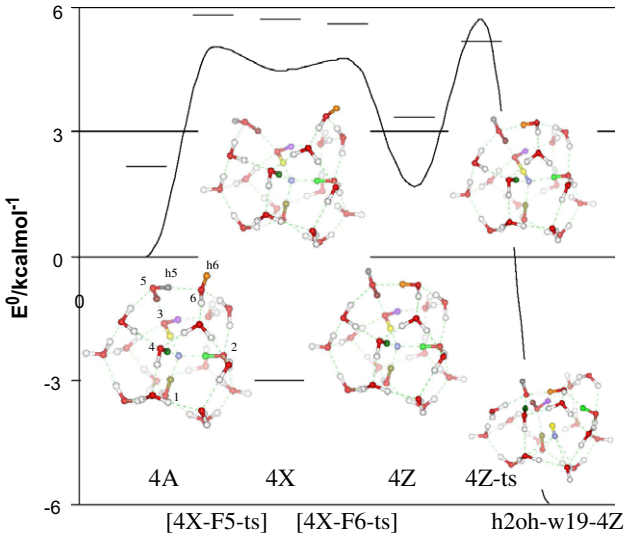

Fig. 8. Selected stationary states on lowest-barrier reaction pathway for h-dod4A. Configuration names are abbreviated by omitting 'h-dod'.

Table 2
Dipole moment (Debye), B3LYP electronic energy and free energy (kcal/mol) at 0 K, and H–H⁻ distance (pm), for $(H^-)(H_2O)_{20}$ or $(H_2)(OH^-)(H_2O)_{19}$ cluster stationary states. For each group of structures, '*c*' is the hydride coordination for the initial reactant.

c	Geometry	Dip	E^0	G^0	H	d_{HH}
3	h-dod3A	0.78	4.17	3.15	h1	140
	h-dod3A-ts	1.11	8.09	4.86	h1	92
	h2oh-w19-3A	4.91	−7.31	−12.42	h1	75
4	h-dod4B	7.46	0.22	0.33	h1	148
	h-dod4B-ts	7.04	6.46	3.65	h1	90
	h2oh-w19-4B	7.03	−9.08	−13.32	h1	75
4	h-dod4A	7.43	0.00	0.00	h1	150
	h-dod4A-ts[h1]	7.59	8.38	5.44	h1	83
	h2oh-w19-4A[h1]	4.52	−3.12	−5.40	h1	74
	h-dod4A	7.43	0.00	0.00	h2	151
	h-dod4A-ts[h2]	6.78	8.29	5.19	h2	84
	h2oh-w19-4A[h2]	2.84	−3.88	−7.24	h2	74
	h-dod4A	7.43	0.00	0.00	h3	151
	h-dod4A-ts[h3]	6.85	8.14	5.03	h3	85
	h2oh-w19-4A[h3]	5.40	−4.42	−6.52	h3	74
	h-dod4A	7.43	0.00	0.00	h4	164
	h-dod4A-ts[h4]	11.92	14.73	10.27	h4	81
	h2oh-w19-4A[h4]	6.02	−2.64	−6.00	h4	74
	h-dod4X-F5-ts	8.17	5.05	3.68	h3	147
	h-dod4X	8.42	4.49	3.56	h3	147
	h-dod4X-F6-ts	8.36	4.76	3.45	h3	146
	h-dod4Z	9.61	1.68	1.23	h3	143
	h-dod4Z-ts	8.93	5.72	3.04	h3	93
	h2oh-w19-4Z	9.93	−5.98	−8.99	h3	74
5	h-dod5A	4.82	0.76	1.27	h1	161
	h-dod5A-ts[h1]	4.22	11.50	8.17	h1	83
	h2oh-w19-5A[h1]	4.80	−1.86	−3.61	h1	74
	h-dod5A	4.82	0.76	1.27	h2	165
	h-dod5A-LH-ts	4.76	2.46	2.54	h2	147
	h-dod5A-LH	5.15	2.36	2.73	h2	144
	h-dod5A-ts[h2]	6.00	6.70	4.56	h2	93
	h2oh-w19-5A[h2]	6.69	−1.03	−3.94	h2	75
6	h-dod6A	4.02	3.10	3.81	h1	174
	h-dod6A-ts	3.57	10.13	7.58	h1	93
	h2oh-w19-6A	5.96	−6.90	−11.41	h1	74

limiting step is the first one, with barrier $\Delta G^{ts} = 3.68$ kcal/mol at 0 K, but above approximately 190 K the h-dod4Z-ts barrier becomes the higher one. At 25 °C, G(h-dod4Z-ts) – G(h-dod4A) = 2.93 kcal/mol.

5.4. Crude stability estimates

The h-dod4A and h-dod5A clusters may be detectable in a low temperature experimental system. Below 125 K, "hopping" and "turning" in ice essentially ceases, and interior proton positions in ice become frozen [56–58]. Wooldridge and Devlin [58] observed ice surface activity to cease below approximately 80 K.

Accurate prediction of reaction rates is a complex enterprise beyond the scope of this article. Reaction rates will be influenced by the quantum nature of both the hydride proton and the solvating protons. For an answer within an order of magnitude or so, the Arrhenius formula

$$\rho = \text{reaction rate} = \frac{RT}{h} e^{-(\Delta G^{ts}/RT)} \tag{4}$$

applied to the h2 simple pathway of h-dod5A gives a mean survival time of $1/\rho = 0.73$ ms at 77 K and 13 ps at 25 °C. For h-dod4A, the three-state system h-dod4A ↔ h-dod4Z → (product) is modeled as a Poisson process, with conversion rates computed using (4). The mean time to formation of H_2 is 6 ms at 77 K and 37 ps at 25 °C. Below 35 K both clusters should be stable for years. As one benchmark, Formula (4) applied to cyclic proton transfer in the water tetramer at 298 K gives a rate of $\rho = 0.7\ s^{-1}$, in good agreement with the rate of $\rho \approx 1\ s^{-1}$ as computed by Loerting et al. [59].

5.5. Ab Initio molecular dynamics

During our 25 ps simulation of H^- in water at 300 K, reaction of H^- with water to form H_2 did not occur. The closest that any water proton came to the hydride was 93 pm. At the point of closest approach, the H^- was 4-coordinated, the nearest solvating proton ('h61') was stretched 118 pm from its O (denoted 'o31'), and another solvating proton ('h39') was 172 pm from the H^- and 233 pm from o31. These distances suggest that h39 "almost" enacted a Laage–Hynes move to o31 but then backed off. A completed Laage–Hynes move for this configuration would probably have led to reaction. The pair correlation functions $g_H(r)$ and $g_O(r)$, between the H^- anion and the water proton and oxygen sites, are depicted in Fig. 9. The $g_H(r)$ curve exhibits a sharp peak centered at 148 pm. Integration of this peak to the first minimum at 235 pm yields 4.04 solvating water molecules as the average coordination number.

To illustrate the trajectory without drowning in data, we sampled every 100th time step (1000 snapshots) and selected only those protons which at some point came within 260 pm of the hydride. The result is shown as Fig. 10. Initially, protons h2, h4, h6, h8 formed the first shell. At $t = 0.64$, h39 joined the inner shell, and h8 left but bounced right back. The hydride stayed 5-coordinated for 1.0 ps and then ejected h6. The only other first-shell exchange oc-

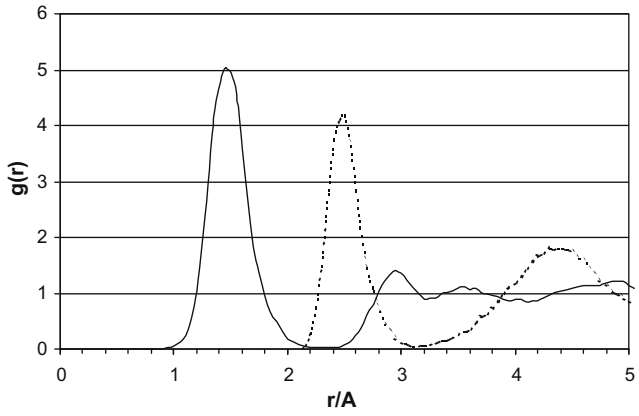

Fig. 9. Proton-hydride (solid) and oxygen-hydride (dotted) correlation functions.

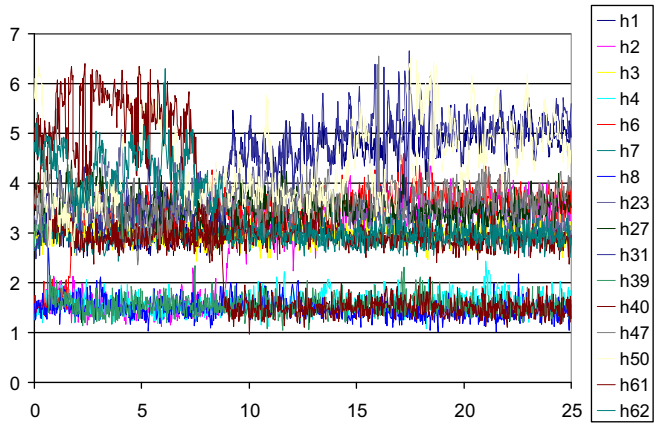

Fig. 10. Hydride-proton distance (A) vs. time (ps) for 16 of 64 protons in AIMD simulation.

curred when h61 arrived at $t = 8.7$ and 0.2 ps later h2 departed. Other forays to 3- or 5-coordinated status were briefer than 100 fs and did not involve exchange. The coordination was 4 at 95% of time steps.

Fig. 10 is qualitatively reminiscent of other anions' hydration behavior [19,60] and is consistent with a Poisson distribution for arrival and departure events. Assuming a Poisson distribution, the average dwell time for each first shell water is 48 ps (95% confidence interval is 20–117 ps). The mean survival time τ of solvated hydride in 300 K water cannot be directly estimated from the simulation since reaction did not occur, but survival through a single 25 ps run puts the 95% confidence lower bound for τ at 8.3 ps. Since reaction "almost" occurred once during this interval and the energetic calculation yielded 37 ps as a ballpark, τ is probably between 20 and 100 ps. Comparisons between these results and those of Heuft and Meijer for fluoride [19] are interesting and are summarized as Table 3.

We acknowledge there are multiple limitations inherent in the use of the PBE functional to make aqueous phase reaction rate predictions. For AIMD simulations using PBE, scaling the temperature up to T ~ 400 K yields better agreement with experimental pair correlation functions and diffusive properties [61–64]. However, a higher temperature will raise the rate of first shell H_2O exchange and will also dramatically accelerate the formation of H_2 and OH^-. We repeated the simulation at 400 K and produced H_2 in 4 ps (and had one exchange event). Furthermore, the PBE functional applied in AIMD simulations tends to overestimate the extent of electron delocalization near the transition state region and hence underestimates the reaction barrier. Other weaknesses of this AIMD simulation are the use of deuterium mass and a thermostat, ignoring zero point motion, and reporting just a single trajectory. Nevertheless, the dynamical behavior observed in the trajectory is evocative and reinforces the conclusions reached in our static *ab initio* cluster calculations.

Table 3
Comparison of AIMD simulations for aqueous fluoride (Ref. [17]) and hydride.

	F^-	H^-
Functional used	BLYP	PBE
Duration, excl. equil. (ps)	18.3	25
Time step (fs)	0.145	0.25
Temp. (K)	300	300
Number of H_2O's	64	32
Cube edge (Å)	12.5	9.86
$g_H(r)$ 1st peak (pm)	166	148
$g_O(r)$ 1st peak (pm)	266	248
$g_H(r)$ 1st trough (pm)	260	235
Closest X^-–H (pm)	130	93
Modal c in simulation	5	4
Mean c in simulation	5.0	4.0
c For lowest $X^-(H_2O)_{20}$	5	4
Number of 1st shell exchanges	6	2
Mean dwell time (ps)	16	48
Dwell time, 95% c.i. (ps)	9–29	20–117
Reaction time (ps)	n.a.	>25

Formula (4) implies that reaction (1) occurs about ten times faster at 400 K than at 300 K, so the 4 ps lifetime at 400 K is consistent with a 40 ps lifetime at 300 K. Taken together, our calculations all point to "tens of picoseconds" as the ballpark for survival time of hydride anion in bulk water at 300 K.

We remark that AIMD studies of water starting from a dodecahedral cage with an enclosed molecule have also been performed for positively charged clusters [65,66]. In these studies, the evolution of $(H_3O^+)(H_2O)_{20}$ at various temperatures was simulated. In addition to the positive rather than negative charge, other differences are that these are models of a finite gas phase cluster rather than bulk water, and the "reaction" being watched for is proton transfer to a different H_2O unit. When H_3O^+ started in the interior of the cluster, proton transfer occurred in the first picosecond [66]. Despite the different setups, Singh's study [65] and ours both found persistence of a 4-coordinated geometry at the central molecule, and the average behavior of the water molecules in the first and second coordination shells were similar in terms of $g(r)$.

6. Conclusion

A lot of interesting chemical dynamics lies behind the simple-looking reaction (1). Despite (1) being highly exothermic, a hydride in a water cluster or aqueous context does not simply grab the nearest water proton. Reaction occurs only when the target H_2O is properly presolvated to release a proton and become hydroxide. In bulk water, this can take tens of picoseconds, which is enough time to sample a huge number of configurations.

Hydride-water interactions offer a possibly unique window into anion solvation dynamics and the importance of the anion solvation hierarchy for controlling a reaction pathway. Small hydride-water clusters are unstable or very short-lived, but kinetic stability is enhanced by encapsulating the hydride and providing more solvation. Our research underscores the importance of topology-energy relationships for water clusters, which we used effectively to locate the longer-lived cluster h-dod4A and to find its lower-barrier reaction pathway via h-dod4Z. The comparison with aqueous fluoride shows some similarities and some differences, including the interesting finding that individual H-bonds to hydride tend to last considerably longer than to fluoride.

Electrolysis is an extremely complex process in which nanostructural factors can make a big difference. If a particular electrode shape and composition were to enable hydrides to form and to become encapsulated by H_2O molecules, the solvated ions might last for tens of picoseconds and their steady-state population might be detectable. This could be true even if the hydride mechanism accounts for only a small fraction of all the electrons conducted into the water phase.

Acknowledgments

Kevin Leung was supported by the Department of Energy under Contract DE-AC04-94AL85000. Sandia is a multiprogram laboratory operated by Sandia Corporation, a Lockheed Martin Company, for the U.S. Department of Energy.

References

[1] Q. Cui, M. Elstner, M. Karplus, J. Phys. Chem. B 106 (2002) 2721.
[2] S. Makoto, Y. Hiroshi, Nippon Kagakkai Koen Yokoshu 86 (2) (2006) 1484.

[3] D.R. Rosseinsky, R.J. Mortimer, Adv. Mater. 13 (2001) 783.
[4] C.A. Kelly, D.R. Rosseinsky, Phys. Chem. Chem. Phys. 3 (2001) 2086.
[5] C. Haertling, R.J. Hanrahan Jr., R. Smith, J. Nucl. Mater. 349 (2006) 195.
[6] J.H. Leckey, L.E. Nulf, J.R. Kirkpatrick, Langmuir 12 (1996) 6361.
[7] J. Phillips, M.C. Bradford, M. Klanchar, Energy Fuels 9 (1995) 569.
[8] H.M. Lee, D. Kim, N.J. Singh, M. Kolaski, K.S. Kim, J. Chem. Phys. 127 (2007) 164311.
[9] T.M. Miller, A.A. Viggiano, A.E. Stevens Miller, R.A. Morris, M. Henchman, J.F. Paulson, J.M. Van Doren, J. Chem. Phys. 100 (1994) 5706.
[10] I. Alkorta, J. Elguero, S.J. Grabowski, J. Phys. Chem. A 112 (2008) 2721.
[11] I. Alkorta, K. Zborowski, J. Elguero, M. Solimannejad, J. Phys. Chem. A 110 (2006) 10279.
[12] S.J. Grabowski, Chem. Phys. Lett. 312 (1999) 542.
[13] S.J. Grabowski, J. Phys. Chem. A 104 (2000) 5551.
[14] L. Perera, M.L. Berkowitz, Z. Phys. D 26 (1993) 166.
[15] J. Baik, J. Kim, D. Majumdar, K.S. Kim, J. Chem. Phys. 110 (1999) 9116.
[16] J. Kim, H.M. Lee, S.B. Suh, D. Majumdar, K.S. Kim, J. Chem. Phys. 113 (2000) 5259.
[17] P. Jungwirth, D.J. Tobias, J. Phys. Chem. B 105 (2001) 10468.
[18] W.H. Robertson, M.A. Johnson, Annu. Rev. Phys. Chem. 54 (2003) 173.
[19] J.M. Heuft, E.J. Meijer, J. Chem. Phys. 122 (2005) 094501.
[20] A. Lenz, L. Ojamäe, Phys. Chem. Chem. Phys. 7 (2005) 1905.
[21] J.-.L. Kuo, C.V. Ciobanu, L. Ojamäe, I. Shavitt, S.J. Singer, J. Phys. Chem. A 118 (2003) 3583.
[22] D.J. Anick, J. Phys. Chem. A 110 (2006) 5135–5143.
[23] D.J. Anick, J. Phys. Chem. A 109 (2005) 5596–5601.
[24] S. Wei, Z. Shi, A.W. Castleman Jr., J. Chem. Phys. 94 (4) (1991) 3268–3270.
[25] T.S. Zwier, Science 304 (2004) 1119–1120.
[26] J.-.W. Shin, N.I. Hammer, E.G. Diken, M.A. Johnson, R.S. Walters, T.D. Jaeger, M.A. Duncan, R.A. Christie, K.D. Jordan, Science 304 (2004) 1137–1140.
[27] D.W. Davidson, in: Felix Franks (Ed.), Clathrate Hydrates; Ch. 3 of Water: A Comprehensive Treatise, second ed., vol. 2, Plenum Press, New York, 1976.
[28] C.A. Koh, Chem. Soc. Rev. 31 (2002) 157–167.
[29] PQS v. 3.1, Parallel Quantum Solutions, 2013 Green Acres Road, Fayetteville, AR 72703.
[30] H.B. Schlegel, J. Chem. Soc., Faraday Trans. 90 (1994) 1569–1574.
[31] S.S.-.L. Chiu, J.J.W. McDougall, I.H. Hillier, J. Chem. Soc., Faraday Trans. 90 (1994) 1575.
[32] P.Y. Ayala, H.B. Schlegel, J. Chem. Phys. 107 (2) (1997) 375–384.
[33] M. Swart, F.M. Mickelhaupt, J. Chem. Theor. Comput. 2 (2006) 281–287.
[34] G. Kresse, J. Furthmuller, Phys. Rev. B 54 (1996) 11169; Comput. Mater. Sci. 6 (1996) 15.
[35] J.P. Perdew, K. Burke, K.M. Ernzerhof, Phys. Rev. Lett. 77 (1996) 3865.
[36] P.E. Blochl, Phys. Rev. B 50 (1994) 17953.
[37] G. Kresse, D. Joubert, Phys. Rev. B 59 (1999) 1758.
[38] J. Melin, J.V. Ortiz, J. Chem. Phys. 127 (2007) 014307.
[39] H.M. Lee, D.J. Anick, K.S. Kim, Int. J. Quantum Chem. 109 (2009) 1820–1826.
[40] D.J. Wales, T.R. Walsh, J. Chem. Phys. 106 (1997) 7193–7207.
[41] D. Sabo, Z. Bačić, J. Chem. Phys. 109 (13) (1998) 5404–5419.
[42] S. Graf, S. Leutwyler, J. Chem. Phys. 109 (13) (1998) 5393–5403.
[43] F.N. Keutsch, J.D. Cruzan, R.J. Saykally, Chem. Rev. 103 (2003) 2533–2577.
[44] M.R. Viant, J.D. Cruzan, D.D. Lucas, M.G. Brown, K. Liu, R.J. Saykally, J. Phys. Chem. A 101 (1997) 9032–9041.
[45] J.D. Cruzan, M.R. Viant, M.G. Brown, R.J. Saykally, J. Phys. Chem. A 101 (1997) 9022.
[46] J.K. Gregory, D.C. Clary, J. Chem. Phys. 105 (16) (1996) 6626–6633.
[47] K. Liu, M.G. Brown, J.D. Cruzan, R.J. Saykally, J. Phys. Chem. A 101 (1997) 9011–9021.
[48] J.J. Finnerty, C. Wentrup, J. Org. Chem 69 (2004) 1909–1918.
[49] D. Laage, J. Hynes, Science 311 (2006) 832.
[50] M.E. Tuckerman, D. Marx, M. Parrinello, Nature (London) 417 (2002) 925–929.
[51] M.E. Tuckerman, A. Chandra, D. Marx, Acc. Chem. Res. 39 (2006) 151–158.
[52] D.E. Smith, L.X. Dang, J. Chem. Phys. 101 (1994) 7873.
[53] J. Sadlej, Chem. Phys. Lett. 333 (2001) 485–492.
[54] D.J. Anick, J. Mol. Struct. (Theochem) 587 (2002) 87–96.
[55] D.J. Anick, J. Mol. Struct. (Theochem) 587 (2002) 97–110.
[56] M. Fisher, J.P. Devlin, J. Phys. Chem. 99 (1995) 11584.
[57] H.H. Richardson, P.J. Wooldridge, J. Phys. Chem. 89 (1985) 3552.
[58] P.J. Wooldridge, J.P. Devlin, J. Chem. Phys. 88 (5) (1988) 3086.
[59] T. Loerting, K.R. Liedl, B.M. Rode, J. Chem. Phys. 109 (7) (1998) 2672–2679.
[60] K. Leung, S.B. Rempe, J. Am. Chem. Soc. 126 (2004) 344.
[61] D. Asthagiri, L.R. Pratt, J.D. Kress, Phys. Rev. E 68 (2003) 041505.
[62] J.G. Grossman, E. Schwegler, E.W. Draeger, F. Gigy, G. Galli, J. Chem. Phys. 120 (2004) 300.
[63] E. Schwegler, J.C. Grossman, F. Gygi, G. Galli, J. Chem. Phys. 121 (2004) 5400.
[64] S.B. Rempe, T.R. Thomas, K. Leung, Phys. Chem. Chem. Phys. 10 (2008) 4685.
[65] N.J. Singh, M. Park, S.K. Min, S.B. Suh, K.S. Kim, Angew. Chem. Int. Ed. 45 (2006) 3795.
[66] S.S. Iyengar, M.K. Petersen, T.J.F. Day, C.J. Burnham, V.E. Teige, G.A. Voth, J. Chem. Phys. 123 (2005) 084309.